IECMS 2018

sciforum

Conference Proceedings Paper

First Zunyite-Bearing Lithocap in Greece: The Case of Konos Hill Mo-Re-Cu-Au Porphyry System

Constantinos Mavrogonatos [1,*], Panagiotis Voudouris [1], Paul G. Spry [2], Vasilios Melfos [3], Stephan Klemme [4], Jasper Berndt [4], Robert Moritz [5] and Christos Kanellopoulos [1]

[1] Faculty of Geology & Geoenvironment, National and Kapodistrian University of Athens, 157 72 Athens, Greece; voudouris@geol.uoa.gr (P.V.); ckanellopoulos@gmail.com (C.K.)
[2] Department of Geological and Atmospheric Sciences, Iowa State University, Ames, IA 50011, USA; pgspry@iastate.edu
[3] Faculty of Geology, Aristotle University of Thessaloniki, 541 24 Thessaloniki, Greece; melfosv@geo.auth.gr
[4] Institut für Mineralogie, Westfälische Wilhelms-Universität Münster, 48149 Münster, Germany; Stephan.Klemme@uni-muenster.de (S.K.); jberndt@uni-muenster.de (J.B.)
[5] Department of Earth Sciences, University of Geneva, 1205 Geneva, Switzerland; Robert.Moritz@unige.ch
* Correspondence: kmavrogon@geol.uoa.gr; Tel.: +30-698-860-8161

Abstract: The Konos Hill prospect, represents a telescoped Mo-Re-Cu-Au porphyry system overprinted by a high sulfidation event. Porphyry mineralization is exposed in the deeper parts of the study area and comprises quartz stockwork veins, hosted in subvolcanic bodies of granodioritic composition. In the upper topographic levels, a significant hydrothermal alteration overprint predominates, and consists of silicification and various advanced argillic alteration assemblages, related to N-S and E-W trending faults. Further outwards, advanced argillic alteration gradually evolves into phyllic assemblages dominated by sericite. Zunyite, described for the first time from a lithocap in Greece, along with various amounts of quartz, alunite, APS minerals, kaolinite, pyrophyllite and diaspore constitute the major advanced argillic alteration minerals in the area. Mineral-chemical analyses revealed significant variance in the SiO_2, F and Cl content of zunyite. Alunite supergroup minerals display a wide compositional range corresponding to members of the alunite, beudantite and plumbogummite subgroups. Diaspore displays almost stoichiometric composition with traces of TiO_2, BaO, Ce_2O_3 and Nd_2O_3. The presence of the above-mentioned minerals indicates that low pH hydrothermal fluids flowing through fault planes resulted in extensive advanced argillic alteration in the area. The discovery of zunyite points towards an enrichment of volatile elements like F and Cl in the hydrothermal fluid, and helps to set constrains on the physicochemical conditions and the evolution of the mineralization and associated alteration.

Keywords: zunyite; lithocap; porphyry-epithermal mineralization; Greece

1. Introduction

Zunyite [$Al_{13}Si_5O_{20}(OH,F)_{18}Cl$] is a rare F- and Cl-bearing, aluminosilicate that was originally described from and named after the Zuni Mine, Anvil Mountain, CO, USA [1]. Its complicates structure has long been the subject of controversy (e.g., [2]), as it is one of the few minerals that are known to contain three different volatile components, namely H_2O, F and Cl [3]. Zunyite has been recognized as a rare mineral in advanced argillic alteration assemblages, which commonly develop in shallow levels, above porphyry Cu-Au deposits (e.g., Lepanto Far Southeast, Philippines [4]) and form from acidic fluids that arise from the condensation of volatiles over the porphyry intrusives [5]. In many cases, advanced argillic alteration zones, or "lithocaps", as were named by Sillitoe (1989) [6], are a favorable environment for exploration, as they may host significant high-sulfidation ores and

adjacent porphyry-style mineralization [7,8]. Commonly, advanced argillic alteration lithocaps comprise various amounts of quartz, andalusite, pyrophyllite, topaz, kaolinite-dickite, diaspore, corundum, zunyite, alunite supergroup minerals, and dumortierite [9–11]. Lithocaps are usually zoned: deep-level assemblages comprise quartz and pyrophyllite, whereas in shallower levels, quartz and alunite predominate and reflect the cooling and increasing acidity of the hydrothermal fluids [12].

Advanced-argillic alteration lithocaps have been described from a number of porphyry/epithermal deposits and prospects in Greece [13,14]. The most well-known examples are Kassiteres-Sapes [15,16], Mavrokoryfi [17] and Melitena [15,18] prospects in Thrace district, northern Greece, as well as the Fakos and Stypsi prospects, in Limnos and Lesvos Islands, respectively [19–21]. Until now, no zunyite has been found in any of these lithocaps and its only occurrence in Greece was reported from advanced argillic-altered rhyolite in Kos Island [22]. We report here the first occurrence of zunyite related to a lithocap over a porphyry system in Greece.

2. Materials and Methods

Twenty rock samples were collected from the advanced argillic-altered rocks of the Konos Hill area for petrographic, mineralogical, and mineral-chemical studies. From these samples, sixteen thin sections underwent detailed petrographical investigation using optical microscopy. Powders from ten representative samples were processed by X-ray diffraction, using a Brooker (Siemens) 5005 X-ray diffractometer, in conjunction with the DIFFRACplus software, at the Faculty of Geology and Geoenvironment, National and Kapodistrian University of Athens. Results were evaluated using the EVA 10.0 software. Chemical compositions of the minerals were determined using electron probe micro-analysis (EPMA) with a JEOL 8530F instrument at the Institute of Mineralogy, University of Münster, Germany. Analytical conditions were: 15 kV accelerating voltage, 5 nA beam current and counting times of 10 s for peak and 5 s for the background signal. Natural (for Na, Mg, Al, Si, Mn, Fe, Sr, Cl, Ba, K, Ca, P and S) and synthetic (for F, Ti, Cr, La, Ce, Nd and Pb) mineral standards were used for calibration prior to quantitative analyses. The phi-rho-z correction was applied to all data and error on major oxides is within 1–2%.

3. Regional and Local Geology

The Rhodope Massif in northern Greece is characterized by Late Cretaceous-Tertiary, syn- to post-orogenic collapse, which exhumed deep-seated metamorphic sequences along major detachment faults and created a number of E-W trending tectonic basins [23,24]. These basins comprise thick, Eocene-Oligocene clastic sequences and basic-to-acidic volcanic rocks. Calc-alkaline to shoshonitic and ultra-potassic plutons and subvolcanic bodies of Oligocene to Miocene age, display supra-subduction geochemical and isotopic signatures [25] and form intrusive bodies in the above-mentioned lithologies. In the Sapes-Kassiteres district, lithologies of the Circum Rhodope Belt crop out, especially in its southern part, with metasedimentary lithologies of the Makri unit being the most widespread. Extended outcrops of the Eocene volcanosedimentary sequence discordantly overlie the metamorphic basement and occupy most of the study area, along with hydrothermally-altered subvolcanic intrusions. Konos Hill, its most prominent topographic feature, is located approximately 20 km N-NW of Alexandroupolis and consists of a hydrothermally-altered granodiorite which intruded into the volcanosedimentary sequence (Figure 1). Further to the E-NE part of the study area, a monzodioritic body intruded into the volcanosedimentary sequence and the granodiorite. Available geochronological data for the monzodiorite yielded cooling ages of 31.9 ± 0.5 Ma (Rb/Sr on biotite, [26]) and 32.6 ± 0.5 Ma ($^{40}Ar/^{39}Ar$ on biotite, [27]). Recently, Perkins et al., 2018 [28] based on U-Pb zircon geochronology, provided additional geochronological data for the broader Kassiteres magmatic suite, that display a time interval between 32.05 ± 0.02 and 32.93 ± 0.02 Ma. Previous studies in this area have shown that granodiorite hosts the Konos Hill porphyry Cu-Mo-Re-Au porphyry prospect [15,29].

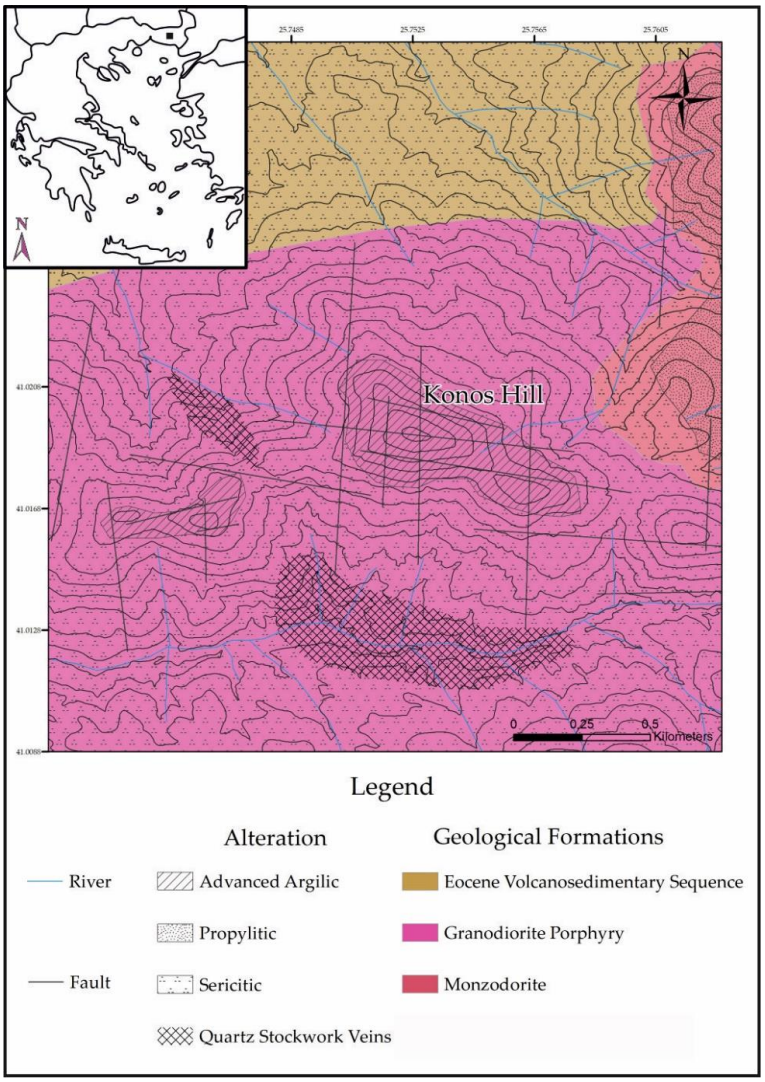

Figure 1. Geological and alteration map of Konos Hill area. Black square in the map of Greece (top-left corner), marks the location of the study area.

4. Alteration and Mineralization

Hydrothermal alteration and mineralization types in the broad Sapes-Kassiteres district, have been well studied [15,16,29–36]. Advanced argillic-altered lithocaps have been so far recognized in a number of occurrences [16]. Among them, Konos Hill is located in the eastern part of this district and comprises the highest topographic level of the area.

Advanced argillic alteration at Konos Hill is related to E-W, N-S and NNW-SSE trending faults and produced a significant overprint of the porphyry-style alteration and mineralization, which is exposed in lower topographic areas (Figure 2a). In the uppermost part, acidic leaching of the granodiorite resulted in a structurally-controlled and spatially restricted silicification zone, which comprises residual and vuggy quartz with minor alunite. Silicified zones grade outwards into advanced argillic assemblages (Figure 2b–e). Adjacent to silicification, alunite + APS minerals + quartz + zunyite ± pyrophyllite assemblages predominate, while more distal assemblages are composed of quartz + alunite + APS minerals + diaspore + kaolinite ± pyrophyllite. The Konos Hill lithocap does not host any significant high-sulfidation ores, apart from pyrite + enargite + colusite, and could be considered as barren, but nearby lithocaps host high-sulfidation, gold-enargite mineralization, which is preferably found in the western part of the study area [15,16,31,35,37–39]. Advanced argillic alteration assemblages evolve through a transitional zone of quartz + alunite +

pyrophyllite + sericite, into a typical sericite-rich assemblage, which is the most widespread type of hydrothermal alteration. Porphyry-style quartz stockwork veins (Figure 2f), hosted in granodiorite, comprise chalcopyrite-pyrite-molybdenite-rheniite mineralization [33] and are associated mostly with sericitic, as well as relics of sodic alteration. Sericitic alteration has also affected extended outcrops of the volcanosedimentary sequence, as well as parts of the monzodiorite intrusion, especially along fault planes. It grades further outwards into propylitic alteration, dominated by varying amounts of epidote, chlorite, and carbonates.

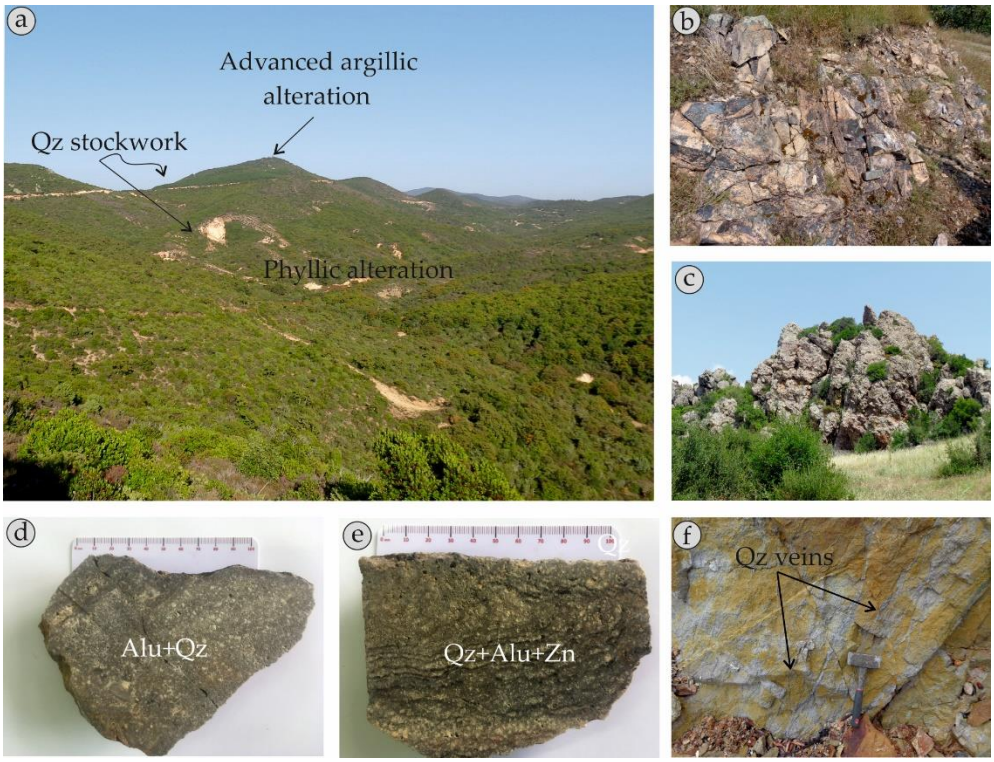

Figure 2. Field and hand-specimens photographs: (**a**) Panoramic view of Konos Hill; (**b**) Quartz-alunite-zunyite bearing rocks on top of Konos Hill; (**c**) Quartz-alunite-diaspore bearing in the NW slopes of Konos Hill; (**d**,**e**) Hand-specimens of quartz-alunite and quartz-alunite-zunyite assemblages; (**f**) Quartz porphyry stockwork veins in sericitic-altered granodiorite (Saporema Creek).

5. Mineralogy and Mineral Chemistry

5.1. Zunyite

Zunyite forms euhedral crystals up to 300 μm in size (Figure 3a,b). They are commonly associated with quartz and tabular alunite-natroalunite crystals, with minor amounts of spheroidal hematite, which along with goethite formed after earlier weathered pyrite. In rare cases, zunyite contains tiny quartz inclusions (Figure 4a,b). Electron probe microanalyses revealed a significant compositional variation (Table 1). SiO_2 varies from 22.7 to 25.14 wt %, whereas the Al_2O_3 content remains fixed (54.97–55.81 wt %). Fluorine and chlorine content varies between 4.07–5.93 wt % and 2.72 to 2.97 wt %, respectively. In some cases, traces of BaO, TiO_2, Na_2O_3 and Ce_2O_3 were detected (up to 0.23, 0.40, 0.26 and 0.34 wt %, respectively).

Table 1. Representative EPM compositions of zunyite (1–6) and diaspore (7–10) from the advanced argillic alteration zone of Konos Hill area.

Wt %	**1**	**2**	**3**	**4**	**5**	**6**	**7**	**8**	**9**	**10**
SiO_2	25.14	22.96	23.66	24.35	22.70	24.58	bd	bd	bd	bd
TiO_2	0.04	0.11	bd	0.26	bd	bd	0.18	bd	bd	bd
Al_2O_3	55.03	54.97	55.25	54.76	55.81	55.32	83.05	82.58	82.42	82.57
FeO	bd	0.05	0.04	0.16	bd	0.08	bd	bd	bd	bd
Na_2O	0.40	0.11	0.34	0.09	0.39	0.19	0.02	bd	0.02	0.01
BaO	0.11	0.07	0.02	0.03	bd	0.23	0.98	bd	bd	bd
La_2O_3	0.03	bd	bd	bd	bd	0.03	bd	bd	bd	0.34
Ce_2O_3	bd	bd	0.02	0.04	bd	0.34	0.02	0.38	0.24	0.09
Nd_2O_3	bd	bd	0.21	bd	0.07	0.09	0.12	0.30	0.16	0.22
P_2O_5	0.05	0.51	0.27	0.25	0.70	0.11	0.05	bd	0.05	bd
F	5.93	4.56	4.82	4.07	5.08	4.32	bd	0.11	bd	bd
Cl	2.90	2.82	2.97	2.91	2.72	2.75	bd	bd	0.01	bd
Total	89.63	86.16	87.60	86.89	87.49	87.96	84.73	83.42	82.90	83.15
apfu			29.5 (O)					1.5 (O)		
Si	5.013	4.679	4.787	4.895	4.596	4.920	0.000	0.000	0.000	0.000
Ti	0.005	0.017	0.000	0.039	0.000	0.000	0.001	0.000	0.000	0.000
Al	12.931	13.202	13.150	12.976	13.190	12.919	0.994	0.997	0.997	0.996
Fe	0.000	0.009	0.007	0.027	0.000	0.013	0.000	0.000	0.000	0.000
Na	0.016	0.043	0.134	0.033	0.154	0.072	0.000	0.000	0.000	0.000
Ba	0.001	0.005	0.002	0.001	0.000	0.018	0.004	0.000	0.000	0.000
La	0.002	0.000	0.000	0.000	0.000	0.002	0.000	0.000	0.000	0.002
Ce	0.000	0.011	0.002	0.003	0.000	0.027	0.000	0.001	0.001	0.001
Nd	0.000	0.000	0.015	0.000	0.007	0.000	0.001	0.001	0.001	0.001
P	0.008	0.089	0.046	0.043	0.120	0.019	0.000	0.000	0.001	0.000
F	3.224	2.956	2.704	2.305	2.837	2.431	0.000	0.004	0.000	0.000
Cl	0.844	0.860	0.891	0.884	0.817	0.830	0.000	0.000	0.000	0.000

5.2. Diaspore

Diaspore is usually found as euhedral to subhedral grains up to 0.2 cm in length (Figures 3e and 4d). It can form aggregates in the quartz + alunite dominated matrix, or it may be scattered as isolated grains in fissures or cracks in the matrix. Electron microprobe analyses revealed almost stoichiometric compositions with traces of TiO_2, BaO, Ce_2O_3 and Nd_2O_3 (up to 0.18, 0.98, 0.38 and 0.22 wt %, respectively; Table 1).

5.3. Alunite Supergroup Minerals

Alunite supergroup consists of four major subgroups, each one containing a varying number of different members. These subgroups namely are the alunite group (e.g., alunite, natroalunite), the beudantite group (e.g., woodhouseite, svanbergite), the plumbogummite group (e.g., crandalite, florencite), and the dussertite group (e.g., arsenocrandalite, segnitite) [40–43]. All members of the supergroup share in common the formula $DG_3(TX_4)_2(X')_6$. In D site, a tetravalent, trivalent, divalent, monovalent cation or partial vacancy can be found (e.g., Ce, La, Nd, Ca, Sr, Ba, Pb, Na, K, NH_4, H_3O), G site is mainly occupied by trivalent and rarely divalent cations (e.g., Al, Fe^{3+}, Cu^{2+}, Zn^{2+}), and T site contains a hexavalent or pentavalent cation (e.g., S, Cr6+, P, As) or minor Si^{4+}. Finally, X and X′ stand for O, (OH), minor F and possibly H_2O [43].

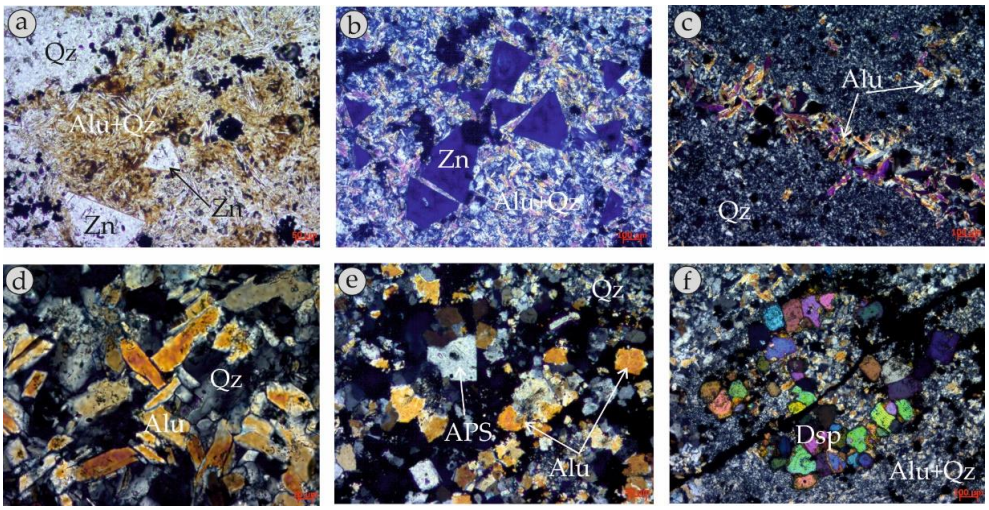

Figure 3. Transmitted light microphotographs of advanced argillic alteration assemblages from the Konos Hill area. (**a**,**b**) Euhedral zunyite (Zn) crystals in association with quartz and tabular alunite (Alu + Qz, // and + nicols respectively); (**c**) Alunite (Alu) vein crosscutting silicified granodiorite (+nicols); (**d**) Tabular alunite crystals in association with quartz (Qz, +nicols); (**e**) APS minerals are found in the core of pseudocubic alunite (+nicols); (**f**) Subhedral diaspore (Dsp) crystals set in an alunite and quartz (Alu + Qz) dominated matrix (+nicols).

Preliminary EPMA revealed significant compositional variations of alunite supergroup minerals in the Konos Hill area. Specifically, analyzed compositions comprise members of the alunite, beudantite, and plumbogummite subgroups as shown in Figure 5a.

APS minerals occur mostly as euhedral pseudocubic inclusions in natroalunite from all types of advanced argillic assemblages at Konos Hill. Most common compositions belong to woodhouseite and strontian woodhouseite with varying amounts of CaO (3.96–7.11 wt %), BaO (up to 1.52 wt %), SrO (up to 9.54 wt %), Ce_2O_3 (up to 1.43 wt %), and P_2O_5 (up to 21.57 wt %). In many cases, traces of TiO_2 (up to 0.15 wt %), La_2O_3 (up to 0.50 wt %), Nd_2O_3 (up to 0.34 wt %), Na_2O (0.61 wt %) and F (up to 0.97 wt %) were detected. Analyzed compositions of APS that plot along the 1:1 line in Figure 5a, display a progressive substitution of PO_4^{3-} by SO_4^{2-}, coupled with substitution of monovalent (K, Na) by divalent (Ca, Ba, Sr) cations in the D site. Compositions that plot further below this line, display a significant variation in P, while the occupancy of D site seems quite stable. This points towards protonation of one of their trivalent anions, in order to establish neutralization. Moreover, those APS minerals that are devoid of monovalent cations (P > 1apfu), are also characterized by a 1:1 substitution in the monovalent-bearing D site by divalent cations (Figure 5b), whereas compositions that plot below this line indicate significant vacancies, due to charge balance.

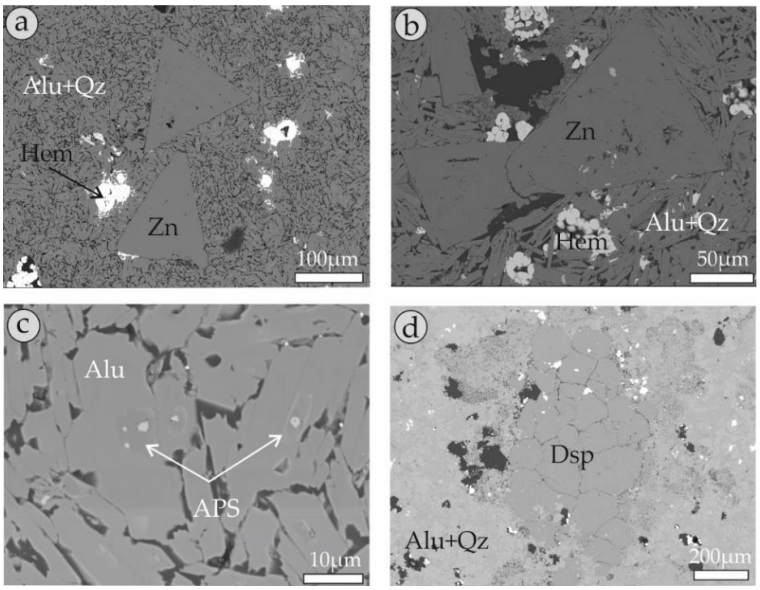

Figure 4. Back-scattered electron microphotographs: (**a**,**b**) Euhedral zunyite (Zn) crystals in association with quartz, tabular alunite (Alu + Qz) and hematite (Hem); (**c**) APS minerals in the core of alunite crystals; (**d**) Diaspore (Dsp) crystals set in an alunite and quartz (Alu + Qz) dominated matrix.

Alunite and natroalunite are the most common representatives of the supergroup and are found in the restricted zone of a vuggy silicification zone, in both quartz + zunyite + kaolinte ± pyrophyllite and quartz + daspore + kaolinite ± pyrophyllite assemblages, as well as in the transitional zone to the sericitic alteration. They are generally found in tabular-shaped or rhombohedral crystals, replacing feldspars or even mafic minerals of the host rock, but pseudocubic shapes were also observed. In other cases, tabular alunites form small veinlets crosscutting the silicified matrix. The majority of alunites are K-rich, with K_2O values reaching up to almost 9 wt %. Na-rich alunite is also common and usually forms euhedral, tabular-shaped crystals with sizes up to 500 μn. In this case, Na_2O content is higher than K_2O and is up to 5.12 wt %, but there are crystals where intense zoning is present as shown by alternations of concentric K- and Na-rich areas in the crystal. Many alunites, especially the tabular-shaped natroalunites can include a core of APS mineral, commonly woodhouseite.

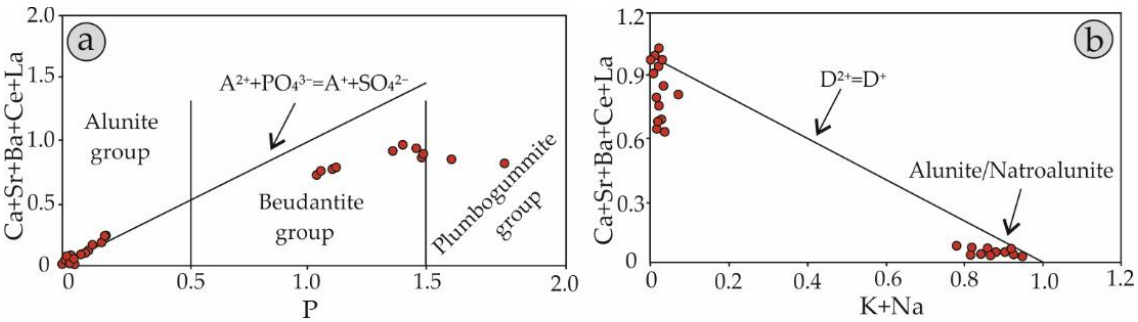

Figure 5. Chemical variation diagrams of analyzed alunite and APS minerals from Konos Hill area: (**a**) Ca + Sr + Ba + Ce + La vs. P plot (marked line represents the occupancy of divalent and trivalent cations in A site, relative to trivalent anions in X site); (**b**) Ca + Sr + Ba + Ce + La vs. K + Na plot (marked line represents occupancy of monovalent relative to divalent cations in D site).

Table 2. Representative EPM compositions of alunite-natroalunite (1–6) and APS minerals (7–10) from the advanced argillic alteration zone of Konos Hill area.

Wt %	1	2	3	4	5	6	7	8	9	10
Al_2O_3	37.90	37.66	39.29	34.54	37.19	37.40	31.59	34.10	34.22	32.78
FeO	0.46	0.30	0.86	0.12	0.28	0.17	0.09	0.06	bd	Bd
CaO	0.01	0.02	0.26	0.38	0.03	0.07	3.96	3.36	7.11	5.94
Na_2O	4.63	5.12	2.21	3.07	4.58	5.01	0.61	0.28	0.08	0.12
K_2O	3.52	3.59	1.65	4.91	3.90	3.41	1.48	0.37	0.21	0.43
BaO	0.15	0.37	0.91	0.21	0.10	0.21	1.47	1.52	0.87	0.97
La_2O_3	0.09	0.08	0.18	0.03	0.37	0.25	0.50	0.07	bd	bd
Ce_2O_3	0.11	0.02	0.48	bd	0.13	0.11	1.42	0.32	bd	bd
Nd_2O_3	bd	bd	0.31	0.28	bd	0.08	0.10	0.34	0.09	bd
SrO	0.01	0.06	0.05	0.31	0.08	0.20	7.83	9.54	7.63	7.82
PbO	bd	bd	bd	bd	bd	bd	bd	bd	bd	0.04
SO_3	34.74	35.16	34.64	34.05	34.24	34.57	15.33	14.35	11.81	12.19
P_2O_5	bd	bd	bd	bd	bd	bd	15.72	17.35	21.57	20.55
Total	81.62	82.38	80.94	78.90	80.90	81.48	80.10	81.61	83.59	80.84
apfu					11 (O)					
Al	3.218	3.177	3.601	3.006	3.197	3.190	3.022	3.134	3.037	2.996
Fe	0.03	0.02	0.05	0.01	0.02	0.01	0.007	0.004	0.000	0.000
Ca	0.00	0.001	0.020	0.029	0.002	0.005	0.298	0.282	0.574	0.488
Na	0.646	0.708	0.289	0.424	0.649	0.704	0.096	0.042	0.011	0.012
K	3.524	3.588	1.651	4.907	3.895	3.411	0.153	0.036	0.019	0.04
Ba	0.004	0.010	0.046	0.006	0.002	0.004	0.047	0.046	0.027	0.029
La	0.002	0.002	0.004	0.001	0.001	0.002	0.015	0.002	0.000	0.000
Ce	0.003	0.001	0.010	0.000	0.003	0.002	0.042	0.010	0.000	0.000
Nd	0.000	0.000	0.007	0.006	0.000	0.000	0.003	0.010	0.002	0.000
Sr	0.000	0.000	0.004	0.016	0.000	0.000	0.368	0.433	0.333	0.340
Pb	0.000	0.000	0.000	0.000	0.000	0.000	0.000	0.000	0.000	0.001
S	1.878	1.886	1.789	1.804	1.879	1.891	0.934	0.841	0.678	0.702
P	0.000	0.000	0.000	0.000	0.000	0.000	1.081	1.148	1.376	1.602

5.4. Kaolinite-Pyrophyllite

Kaolinite and pyrophyllite are present as minor constituents in the studied alteration types. They usually form small, acicular aggregates that accompany quartz-alunite-APS-diaspore and quartz-alunite-zunyite-APS assemblages. Their presence, beyond microscopic examination was verified by X-ray diffraction patterns (Table 3).

Table 3. Mineralogical content of advanced argillic-altered samples defined by XRD analyses.

Sample	Quartz	Alunite	Zunyite	Pyrophyllite	Kaolinite	Diaspore
1	+++	+				
2	+++	++	+		+	
3	++	+++				
4	++	++		+		
5	+++	+				+
6	+++	++		+		
7	+++	++				
8	++	+++				
9	+++	++			+	
10	+++	++		+	+	

6. Discussion and Conclusions

Zunyite-bearing assemblages in lithocaps above porphyry systems have previously been recognized (e.g., Mi Vida porphyry copper system, Argentina, [44]), and in altered aluminous shales, close to manganese deposits [45]. Since then, zunyite has been recognized from a number of porphyry/epithermal deposits (e.g., Hugo Dumett porphyry Cu-Au deposit, Oyu Tolgoi, Mongolia, [46]; Aqua Rica, Catamarca, Argentina, [47]; Chelopech HS Cu-Au deposit, Bulgaria, [48]; Rosia Poieni Cu deposit, Apuseni mountains, Romania, [49]) as a minor constituent in advanced argillic alteration assemblages. These types of hypogene advanced argillic alteration assemblages are believed to form over subvolcanic intrusions from disproportionating magmatic volatiles that derive from a crystallizing melt [4].

Advanced argillic lithocaps form in higher topographic levels, from magmatic gases, contemporaneously with the formation of porphyry-style alteration and mineralization at depth [4]. Field and mineralogical data from the Konos Hill area, strongly support the idea of hypogene formation of the advanced argillic alteration which is in agreement with the findings of Voudouris (2014) [16], who described similar assemblages from the nearby occurrences of advanced argillic altered rocks in the broader Sapes-Kassiteres district. Mineralogical differences that were identified in the studied occurrence, may be due to different degrees of hydrothermal alteration. The occurrence of both advanced argillic and transitional to sericitic alteration zones in the Konos Hill area is similar to other analogous porphyry/epithermal transition environments (e.g., Lepanto-Far Souheast, Philippines, [4]; Asarel porphyry Cu deposit, Bulgaria, [50]). The presence of zunyite in a lithocap that overlies a porphyry deposit, is described here for the first time and constitutes the second occurrence of this mineral in Greece, beyond the advanced argillic altered rhyolite of Kos Island [22]. Its occurrence suggests the availability of F and Cl in the hydrothermal fluid, which resembles the results of Voudouris (2018), who described a topaz-bearing advanced argillic assemblage from the nearby Koryphes Hill area. Estimations of the temperature of formation of zunyite formation in the Konos Hill area is below 450 °C, based on the fact that at this temperature, zunyite is replaced by topaz [51]. A low-temperature limit could be set by the coexistence of zunyite with pyrophyllite, which according to Reyes (1990, 1991) [52,53], does not form below 200 °C. Thus, zunyite probably formed between 200 and 450 °C. A more restrictive T range of 280–350 °C for its formation is based on the similarity of zunyite-bearing assemblages at Konos Hill with those observed in the Hugo Dummet porphyry Cu-Au deposit [46] which formed at this range of temperatures. Further constraints can be made on the fact that the studied assemblages contain alunites that include APS minerals, which according to Hedenquist et al. (1998) [4], formed in a high-temperature environment, at the margins of a magmatic intrusion, compared to APS-free alunites. Finally, the fact that advanced argillic zones in the area of Konos Hill display a more-or-less E-W trending symmetry, that follows the major tectonic line of granodiorite emplacement, suggests that the low pH hydrothermal fluids from which advanced argillic alteration assemblages were derived, were channeled through fault planes.

Author Contributions: C.M. collected the studied samples. C.M. assisted by S.K. and J.B. acquired the mineral-chemical data and evaluated them along with P.V., P.G.S., V.M., R.M. and C.K. C.M. wrote the manuscript. This paper is part of the first author's PhD thesis.

Acknowledgments: The authors would like to thank Mrs Beatte Schmitte her kind help on microanalyses in the Institute of Mineralogy, University of Münster.

Conflicts of Interest: The authors declare no conflict of interest.

References

1. Kloprogge, J.T.; Frost, R.L. Raman and infrared microscopy study of zunyite, a natural Al13 silicate. *Spectr. Acta* **1999**, *55*, 1505–1513.

2. Zhou, B.; Sherriff, B.L. Nuclear magnetic Resonance study of AL:Si and F:OH order in zunyite. *Can. Miner.* **2003**, *41*, 891–893.
3. Louisnathan, S.J.; Gibbs, G.V. Aluminium-silicon distribution in zunyite. *Am. Miner.* **1972**, *57*, 1089–1108.
4. Hedenquist, J.W.; Arribas, A.; Reynolds, T.J. Evolution of an intrusion-centered hydrothermal system: Far Southeast-Lepanto porphyry and epithermal Cu-Au deposis, Philippines. *Econ. Geol.* **1998**, *93*, 373–404.
5. Hedenquist, J.W.; Lowenstern, J.B. The role of magmas in the formation of hydrothermal ore deposits. *Nature* **1994**, *370*, 519–527.
6. Sillitoe, R.H. Gold deposits in Western Pacific island arc: The magmatic connection. *Econ. Geol. Mon*. **1989**, *6*, 251–298.
7. Sillitoe, R.H. Styles of high-sulphidation gold, silver and copper mineralization in the porphyry and epithermal environments. In Proceedings of the Pacrim '99 Congress, Bali, Indonesia, 10–13 October 1999.
8. Watanabe, Y.; Aoki, M.; Yamamoto, K. Geology, age and style of the advanced argillic alteration in the Kobui area, Southwesterm Hokkaido, Japan. *Res. Geol.* **1997**, *47*, 263–281.
9. Meyer, C.; Hemley, J.J. Wall rock alteration. In *Geochemistry of Hydrothermal ore Deposits*; Barnes, H.L., Ed.; Holt: New York, NY, USA, 1967; pp. 166–235.
10. Stoffregen, R.E.; Alpers, C.N. Woodhouseite and svanbergite in hydrothermal ore deposits: Products of apatite destruction during advanced argillic alteration. *Can. Mineral.* **1987**, *25*, 201–211.
11. Seedorff, E.; Dilles, J.H.; Proffett, J.M.; Einaudi, M.T.; Zurcher, L.; Stavast, W.J.A.; Johnson, D.A; Barton, M.D. Porphyry deposits: Characteristics and origin of hypogene features. *Econ. Geol.* **2005**, *100*, 251–298.
12. Sillitoe, R.H. Porphyry copper systems. *Econ. Geol.* **2010**, *105*, 3–41.
13. Voudouris, P.; Spry, P.G.; Melfos, V.; Alfieris, D.; Mavrogonatos, C.; Repstock, A.; Djiba, A.; Stergiou, C.; Periferakis, A.; Melfou, M. Porphyry and Epithermal Deposits in Greece: A Review and New Discoveries. In Proceedings of the 8th Geochemistry Symposium, Antalya, Turkey, 2–6 May 2018.
14. Melfos, V.; Voudouris, P. Cenozoic metallogeny of Greece and potential for precious, critical and rare metals exploration. *Ore Geol. Rev.* **2017**, *59*, 1030–1057.
15. Voudouris, P.; Tarkian, M.; Arikas, K. Mineralogy of telluride-bearing epithermal ores in Kassiteres-Sappes area, western Thrace, Creece. *Min. Petrol.* **2006**, *87*, 31–52.
16. Voudouris, P. Hydrothermal corundum, topaz, diaspore and alunite supergroup minerals in the advanced argillic alteration lithocap of the Kassiteres-Sapes porphyry-epithermal system, western Thrace, Greece. *Neues Jahr. Min.* **2014**, *191*, 117–136.
17. Voudouris, P. Conditions of formation of the Mavrokoryfi high-sulfidation epithermal Cu-Ag-Au-Te deposit (Petrota Graben, NE Greece). *Min. Petrol.* **2011**, *101*, 97–113.
18. Voudouris, P.; Melfos, V. Aluminum-phosphate-sulfate (APS) minerals in the sericitic-advanced argillic alteration zone of the Melitena porphyry-epithermal Mo-Cu- ± Au ± Re prospect, western Thrace, Greece. *Neues Jahr. Min.* **2013**, *190*, 11–27.
19. Voudouris, P.; Alfieris, D. New porphyry-Cu ± Mo occurrences in northeastern Aegean/Greece: Ore mineralogy and transition to epithermal environment. In *Mineral Deposit Research: Meeting the Global Challenge*; Mao, J., Bierlein, F.P., Eds.; Springer: Berlin, Germany, 2005; pp. 473–476.
20. Fornadel, A.P.; Voudouris, P.; Spry, P.G.; Melfos, V. Mineralogical, stable isotope and fluid inclusion studies of spatially related porphyry Cu-Mo and epithermal Au-Te mineralization, Fakos Peninsula, Limnos Island, Greece. *Min. Petrol.* **2012**, *105*, 85–111.
21. Periferakis, A.; Voudouris, P.; Melfos, V.; Mavrogonatos, C.; Alfieris, D. The Stypsi-Megala Therma porphyry-epithermal mineralization, Lesvos Island, Greece: New mineralogical and geochemical data. *Geophys. Res. Abstr. EGU Gen. Assem.* **2017**, *19*, EGU2017–12950.
22. Papoulis, D.; Tsolis-Katagas, P.; Katagas, C. New find of zunyite in advanced argillic alteration of rhyolites, Kos Island, South Aegean volcanic arc, Greece. *Bull. Geol. Soc. Greece* **2004**, *36*, 474–480.
23. Jolivet, L.; Brunn, J.P. Cenozoic geodynamic evolution of the Aegean Region. *Int. J. Earth Sci.* **2010**, *99*, 109–138.
24. Marchev, P.; Kaiser-Rohrmeier, M.; Heinrich, Ch.; Ovtcharova, M.; von Quadt, A.; Raicheva, R. Hydrothermal ore deposits related to post-orogenic extensional magmatism and core complex formation: The Rhodope Massif of Bulgaria and Greece. *Ore Geol. Rev.* **2005**, *27*, 53–89.
25. Pe-Piper, G.; Piper, D.J.W. Unique features of the Cenozoic igneous rocks of Greece. *Geol. Soc.* **2006**, *409*, 259–282.

26. Del Moro, A.; Innocenti, F.; Kyriakopoulos, C.; Manetti, P.; Papadopoulos, P. Tertiary granitoids from Thrace (Northern Greece): Sr isotopic and petrochemical data. *Neues Jahr. Miner.* **1988**, *159*, 113–135.
27. Ortelli, M.; Moritz, R.; Voudouris, P.; Cosca, M.; Spangenberg, J. Tertiary porphyry and epithermal association of the Sapes-Kassiteres district, Eastern Rhodopes, Greece. In Proceedings of the SEG Conference, Keystone, CO, USA, 2–5 October 2010.
28. Perkins, R.; Copper, F.J.; Condon, D.J.; Tattitsch, B.; Naden, J. Post-collisional Cenozoic extension in the northern Aegean: The high-K to shoshonitic intrusive rocks of the Maronia Magmatic Corridor, northeastern Greece. *Lithosphere* **2018**, doi:10.1130/L730.1.
29. Ortelli, M.; Moritz, R.; Voudouris, P.; Spangenberg, J. Tertiary porphyry and epithermal association of the Sapes-Kassiteres district, Eastern Rhodopes, Greece. In Proceedings of the 10th Biennial SGA Meeting, Townsville, Australia, 17–20 August 2009; pp. 536–538.
30. Michael, C. Geology and geochemistry of epithermal gold deposit in Konos area. *Int. Rep.* **1993**, *75*, 77.
31. Voudouris, P. Mineralogical, Geochemical and Fluid Inclusion Studies on Epithermal Vein Type Gold/Silver Mineralizations at Kassiteres/Sapes, (NE- Greece). Ph.D. Thesis, University of Hamburg, Hamburg, Germany, 1993.
32. Arikas, K.; Voudouris, P. Hydrothermal alterations and mineralizations of magmatic rocks in the southern Rhodope Massif. *Acta Vulc.* **1998**, *10*, 353–365.
33. Voudouris, P.; Melfos, V.; Spry, P.G.; Bindi, L.; Moritz, R.; Ortelli, M.; Kartal, T. Extremely Re-rich molybdenite from porphyry Cu-Mo-Au prospects in northeastern Greece: Mode of occurrence, causes of enrichment, and implications for gold exploration. *Minerals* **2013**, *3*, 165–191.
34. Ortelli, M. Tertiary Porphyry and Epithermal Association of the Sapes-Kassiteres District, Eastern Rhodopes, Greece. Master's Thesis, University of Geneva, Geneva, Switzerland, 2009.
35. Kilias, S.; Naden, J.; Paktsevanoglou, M.; Giampouras, M.; Stavropoulou, A.; Apeiranthiti, D.; Mitsis, I.; Koutles, T.; Michael, K.; Christidis, C. Multistage alteration, mineralization and ore-forming fluid properties at the Viper (Sappes) Au-Cu-Ag-Te ore body, W. Thrace, Greece. *Bull. Geol. Soc. Greece* **2013**, *47*, 1635–1644, doi:10.12681/bgsg.11007.
36. Mavrogonatos, C.; Voudouris, P.; Spry, P.G.; Melfos, V.; Klemme, S.; Berndt, J.; Periferakis, A. Biotite Chemistry from Porphyry-Style Mineralization in Western Thrace, Greece. In Proceedings of the 8th Geochemistry Symposium, Antalya, Turkey, 2–6 May 2018.
37. Bridges, P.S.; Gordon, M.J.; Michael, C.; Ampatzioglou, M. Gold mineralization at Sappes, Northern Greece. *Irish Assoc. Econ. Geol.* **1997**, 95–107.
38. Shawh, A.J.; Constantinides, D.C. The Sappes gold project. *Bull. Geol. Soc. Greece* **2001**, *34*, 1073–1080.
39. Michael, C. Epithermal systems and gold mineralization in Western Thrace, (North Greece). *Bull. Geol. Soc. Greece* **2004**, *36*, 416–423.
40. Jambor, J.L. Nomenclature of the alunite supergroup. *Can. Min.* **1999**, *37*, 1323–1341.
41. Dill, H.G. The geology of aluminium phosphates and sulfates of the alunite group minerals: A review. *Earth Sci. Rev.* **2001**, *53*, 35–93.
42. Mills, S.J.; Harter, F.; Nickel, E.H.; Ferraris, G. The standardization of mineral group hierarchies: Application to recent nomenclature proposals. *Eur. J. Miner.* **2009**, *21*, 1073–1080.
43. Bayliss, P.; Kolitsch, U.; Nickel, E.H.; Pring, A. Alunite supergroup: Recommended nomenclature. *Mineral. Mag*. **2010**, *74*, 919–927.
44. Koykharsky, M.; Mirré, J.C. Mi Vida prospect; a porphyry copper-type deposit in northwestern Argentina. *Econ. Geol.* **1976**, *71*, 849–863, doi:10.2113/gsecongeo.71.5.849
45. Nel, L.T. A new occurrence of zunyite near Potmasburg, South Africa. *Mineral. Mag.* **1930**, *22*, 207–220.
46. Khashgerel, B.; Kavalieris, I.; Ken-Ichiro, H. Mineralogy, textures and whole-rock geochemistry of advanced argillic alteration: Hugo Dumett porphyry Cu-Au deposit, Oyu Tolgoi mineal district, Mongolia. *Econ. Geol.* **2008**, *71*, 849–863, doi:10.2113/gsecongeo.71.5.849
47. Franchini, M.; Impiccini, A.; Lentz, D.; Ríos, F.J.; O'Leary, S.; Pons, J.; Schalamuk, A.I. Porphyry to epithermal transition in the Agua Rica polymetallic deposit, Catamarca, Argentina: An integrated petrologic analysis of ore and alteration parageneses. *Ore Geol. Rev.* **2011**, *41*, 49–74, doi:10.1016/j.oregeorev.2011.06.010.

48. Georgieva, S.; Velinova, N. Alunite from the advanced argillic alterations in the Chelopech high-sulphidation epithermal Cu-Au deposit, Bulgaria: Chemistry, morphology and genetic significance. *Bull. Min. Petr. Geochem.* **2012**, *49*, 17–31.
49. Milu, V.; Milesi, J.-P.; Leroy, J.L. Rosia Poieni copper deposit, Apuseni Mountains, Romania-advanced argillic overprint of a porphyry system. *Min. Dep.* **2004**, *39*, 173–188.
50. Hikov, A.; Lerouge, C.; Velinova, N. Geochemistry of alunite group minerals in advanced argillic altered rocks from the Asarel porphyry copper deposit, Central Srednogorie. *Rev. Bulg. Geol. Soc.* **2010**, *71*, 133–148.
51. Hsu, L.C. Stability relations of zunyite under hydrothermal conditions. *Geol. Soc. Am. Abstr. Programs* **1985**, *17*, 98.
52. Reyes, A.G. Petrology of Philippine geothermal systems and the application of alteration mineralogy to their assessment. *J. Volc. Geother. Res.* **1990**, *43*, 279–309.
53. Reyes, A.G. Mineralogy, distribution and origin of aid alteration in Philippine geothermal systems. *Geol. Surv. Japan Report, Tsukuba,* **1991**.